

AD-A069 046

IRT CORP SAN DIEGO CALIF

F/G 4/1

MEASUREMENTS OF SELECTED CHARGE TRANSFER PROCESSES AT LOW ENERGY--ETC(U)

NOV 78 J A RUTHERFORD, R H NEYNABER

DNA001-77-C-0202

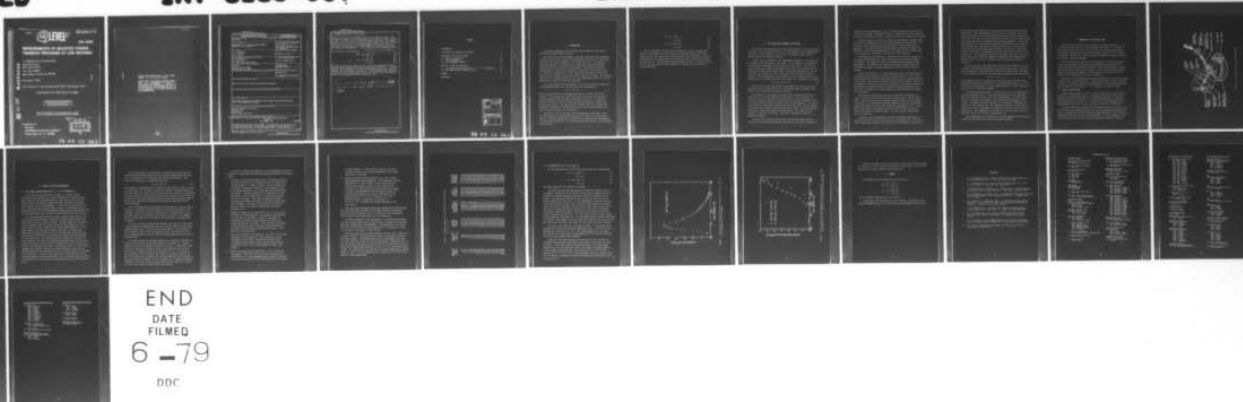
UNCLASSIFIED

IRT-8163-007

DNA-4695F

NL

1 OF 1
AD
A069 046



(12) LEVEL

AD-E300516

DNA 4695F

MEASUREMENTS OF SELECTED CHARGE TRANSFER PROCESSES AT LOW ENERGIES

J. A. Rutherford, R. H. Neynaber,
and D. A. Vroom
IRT Corporation
P. O. Box 80817
San Diego, California 92138

November 1978

Final Report for Period November 1977—November 1978

CONTRACT No. DNA 001-77-C-0202

APPROVED FOR PUBLIC RELEASE;
DISTRIBUTION UNLIMITED.

THIS WORK SPONSORED BY THE DEFENSE NUCLEAR AGENCY
UNDER RDT&E RMSS CODE B322077464 S99QAXHD41110 H2590D.

Prepared for
Director
DEFENSE NUCLEAR AGENCY
Washington, D. C. 20305



79 04 12 033

AD A069046

DDC FILE COPY.

Destroy this report when it is no longer needed. Do not return to sender.

PLEASE NOTIFY THE DEFENSE NUCLEAR AGENCY,
ATTN: TISI, WASHINGTON, D.C. 20305, IF
YOUR ADDRESS IS INCORRECT, IF YOU WISH TO
BE DELETED FROM THE DISTRIBUTION LIST, OR
IF THE ADDRESSEE IS NO LONGER EMPLOYED BY
YOUR ORGANIZATION.



UNCLASSIFIED

SECURITY CLASSIFICATION OF THIS PAGE (When Data Entered)

REPORT DOCUMENTATION PAGE		READ INSTRUCTIONS BEFORE COMPLETING FORM
1. REPORT NUMBER DNA 4695F	2. GOVT ACCESSION NO.	3. RECIPIENT'S CATALOG NUMBER
4. TITLE (and Subtitle) MEASUREMENTS OF SELECTED CHARGE TRANSFER PROCESSES AT LOW ENERGIES		5. TYPE OF REPORT & PERIOD COVERED Final Report for Period Nov 77—Nov 78
7. AUTHOR(s) J. A. Rutherford R. H. Neynaber D. A. Vroom		6. PERFORMING ORG. REPORT NUMBER IRT 8163-007
9. PERFORMING ORGANIZATION NAME AND ADDRESS IRT Corporation P.O. Box 80817 San Diego, California 92138		8. CONTRACT OR GRANT NUMBER(s) DNA 001-77-C-0202
11. CONTROLLING OFFICE NAME AND ADDRESS Director Defense Nuclear Agency Washington, D.C. 20305		10. PROGRAM ELEMENT, PROJECT, TASK AREA & WORK UNIT NUMBERS Subtask S99QAXHD411-10
14. MONITORING AGENCY NAME & ADDRESS (if different from Controlling Office) 62704H		12. REPORT DATE November 1978
		13. NUMBER OF PAGES 30
		15. SECURITY CLASS (of this report) UNCLASSIFIED
		15a. DECLASSIFICATION/DOWNGRADING SCHEDULE
16. DISTRIBUTION STATEMENT (of this Report) Approved for public release; distribution unlimited.		
17. DISTRIBUTION STATEMENT (of the abstract entered in Block 20, if different from Report)		
18. SUPPLEMENTARY NOTES This work sponsored by the Defense Nuclear Agency under RDT&E RMSS Code B322077464 S99QAXHD41110 H2590D.		
19. KEY WORDS (Continue on reverse side if necessary and identify by block number) Charge-Transfer Cross Sections Nitrogen Ions Oxygen Ions Crossed Beam Scattering		
20. ABSTRACT (Continue on reverse side if necessary and identify by block number) Measurement of the charge transfer cross section for the process $N^+ + O_2^+ \rightarrow NO^+ + O$ was completed during the contract year. The experiment was conducted using a crossed beam apparatus. The O^+ atoms were formed in a microwave or rf discharge using pure O_2^+ with traces of H_2O present. Varying the amount of \rightarrow (over)		

UNCLASSIFIED

SECURITY CLASSIFICATION OF THIS PAGE(When Data Entered)

20. ABSTRACT (Continued)

the above

¹⁷H₂O present allowed the dissociation fraction in the O₂⁺ to be varied. This variation was needed to allow determination of the effects of other competing processes. The cross section for reaction (1) was determined in the energy range from 0.5 eV to 12 eV in the center-of-mass system. The signals obtained indicated that this process does not vary rapidly with energy. The cross section was determined to be $1.2 \times 10^{-17} \text{ cm}^2$ at the lowest energies studied and increases to approximately $2.5 \times 10^{-17} \text{ cm}^2$ at 12 eV in the center-of-mass.

Cross sections for the reactions

10 to the -17th power sq cm



were measured during the contract period. The values determined for these processes were essentially the same as those measured previously. In addition, the upper limits determined at energies where these processes have very small probabilities were pushed to lower values. The measurements were undertaken to resolve a conflict between our data and cross section values postulated to explain results obtained in another experiment. ←

Al⁺ + O₂ yields AlO⁺ + O and Al + O₂⁺
and Al⁺ + N₂ yields AlN⁺ + N and Al + N₂⁺

UNCLASSIFIED

SECURITY CLASSIFICATION OF THIS PAGE(When Data Entered)

CONTENTS

1. INTRODUCTION.	3
2. THE PRIMARY AND SECONDARY ION SYSTEMS	5
3. FORMATION OF THE NEUTRAL BEAMS.	8
3.1 THERMAL DISSOCIATION	8
3.2 THE rf DISCHARGE	10
3.3 THE MICROWAVE DISCHARGE.	11
4. RESULTS TO DATE AND DISCUSSION.	12
4.1 THE CHARGE TRANSFER REACTION $N^+ + O \rightarrow N + O^+$ (REACTION 1). . .	12
4.2 THE REACTIONS OF Al^+ WITH O_2 AND N_2	17
5. SUMMARY	20
REFERENCES.	21

ACCESSION for		
NTIS	White Section	<input checked="" type="checkbox"/>
DDC	Buff Section	<input type="checkbox"/>
UNANNOUNCED		<input type="checkbox"/>
JUSTIFICATION _____		
BY _____		
DISTRIBUTION/AVAILABILITY CODES		
Dist.	AVAIL. and/or	SPECIAL
A		

1. INTRODUCTION

This report summarizes results obtained for the Defense Nuclear Agency under Contract Number DNA001-77-C-0202.

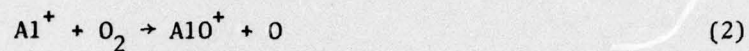
The transmission of electromagnetic radiation through the upper atmosphere continues to be an area of concern to the Department of Defense. In particular, the problem of reliable communication links with satellites is becoming increasingly important as surveillance and communication systems become more sophisticated and our reliance on them develops. The problem of satellite communications is of particular importance at the present time because we are in a period of increased solar activity during which the degree of ionization present in the atmosphere can be significantly higher than average. The resultant scintillation or twinkling effects on satellite communication links can seriously degrade the reliability of the data transmitted.

The charge transfer reaction between N^+ and O is of considerable importance in atmospheric deionization. This reaction can be represented as



One of the major thrusts of the program has been an in-depth study of this reaction. The result of this study is that the cross section for reaction (1) has been measured in the ion energy range from 0.9 to 25 eV. In a previous study of reaction (1) (Ref. 1) we were only able to determine an upper limit for the cross section. The main goal of the present study was to improve the measurement techniques to increase both the size of the signal measured and to lower the detection level of our apparatus.

Reactions of Al^+ with the major neutral atmospheric constituents is the principal mechanism by which these debris ions are slowed. The rate at which they are slowed and the products of reaction are of importance in understanding the role of these particles. As a second task under the contract, we reinvestigated the processes



Where the processes had measurable probabilities in the ion energy range between 1 eV and 5000 eV, cross sections were obtained. Where no detectable signal could be seen, upper limits for the processes were determined. The values determined for these processes were essentially the same as those measured previously (Ref. 2). The measurements were undertaken to resolve a conflict between our data and cross section values postulated to explain results obtained in another experiment.

2. THE PRIMARY AND SECONDARY ION SYSTEMS

The crossed-ion modulated-neutral beam apparatus used in this study has been described in the literature (Refs. 3-5). As a consequence, only an abbreviated description of the instrument is given here. The methods used to form the neutral beams are described in Section 3.

Figure 1 shows a schematic of the experimental apparatus. The primary ions are formed in the source shown in the figure. N^+ was formed in a conventional electron impact bombardment source using an N_2/He gas mixture. The use of a helium "carrier gas" promoted the production of N^+ and tests indicated that the bulk of N^+ was formed with a lower kinetic energy than obtained from a source using pure N_2 . Further use of He in the source favors formation of ground state N^+ . These observations on the formation of N^+ in a N_2/He mixture can be explained if it is assumed that most of the atomic ions are formed in the process



The Al^+ used in task 2 was formed in the primary ion source by a surface ionization process involving $AlCl_3$ and a hot (2800K) tungsten filament. The details of this technique are given in reference 2.

The primary ions are extracted from this source and mass-analyzed at an energy of 75 eV in a 180° magnetic-mass spectrometer. After analysis, the ions pass through an aperture in an iron plate that shields the magnetic field of the mass analyzer from the succeeding regions of the apparatus. The ions are then retarded or accelerated to the desired collision energy, and pass through a field-free region before intersecting the neutral beam. Collimating apertures ensure that, from purely geometrical considerations, all primary ions pass through the modulated neutral beam. The beam is modulated at 100 Hz by mechanical chopping.

Secondary ions resulting from collisions between the primary ions and neutral species are extracted along the direction of the primary ion beam by an

electric field of approximately 2 V/cm. The ions then enter an electric field in which their energy is increased to 1650 eV. Penetration of this accelerating field into the interaction region is reduced by the use of a double-grid structure.

After acceleration, the ions pass through an electrostatic quadrupole lens that forms the entrance slit for a 60°-sector magnetic-mass spectrometer. The mass-selected ions impinge on the first dynode of a 14-stage CuBe electron multiplier. The output from the multiplier passes successively through a pre-amplifier, a 100-Hz narrow-band amplifier, and a phase-sensitive detector, and is then integrated. The output is presented on a chart recorder.

The primary ion beam intensity is measured at the interaction region with an alkadag coated Faraday cup, which can be moved into the collision region when desired. The primary ion energy is determined from retarding potential measurements. All surfaces in the interaction region are gold plated, and the interaction region is normally maintained at 120°C to minimize surface-charging.

Because, for reaction (1), interest extended to small-collision energies, only weak extraction fields at the collision region were used. As a result, the secondary ions were not collected with 100% efficiency. Obtaining absolute cross sections for production of various secondary ions, therefore, required determination of their overall detection efficiency. This latter consideration was governed by a number of factors, including the multiplier gain and the efficiency of transmission of the secondary ions from the interaction region to the multiplier.

The multiplier-amplifier-recorder gain is measured by modulating the primary ions prior to their entry into the collision region. The ion current signal is first measured with the movable Faraday cup and, after traversing the secondary mass spectrometer multiplier-amplifier system, by the recorder. Primary ion transmission through the second mass spectrometer is 92%. Typical gains for the entire system are of the order of 10^{15} output volts on the recorder per ampere of incoming current. In practice, gains are measured for each product ion.

In general, for our experiments, the major experimental uncertainty is associated with the collection efficiency for the secondary ions. Collection fields large enough to ensure total collection of the secondary ions cannot be

used because of the influence these fields exert on the motion of low-energy primary ions. While measurements of the variation of collection efficiency with the strength of the extraction field can readily be made at high primary ion energies, the results are not necessarily relevant to the low-energy regime, where the dynamics of the ion-neutral process may be different. In most cases, interpretation of the data obtained using weak collection fields is based on the assumption that, for primary ion energies above a few eV, the secondary ions are collected with nearly equal efficiency, and that, as a result, the collection efficiency is independent of both the nature and the energy of the primary ions. This assumption implies that the energy defect in the reaction is not large, since energy not expended in excitation of the products must appear as kinetic energy and, therefore, would influence the collection efficiency.

For the particular study being conducted here, another method was used to circumvent the problem of determining the collection efficiently. Here, the signals obtained for reaction (1) were placed on an absolute scale by comparison of the signal size for that reaction with the signal size for the reaction



This accidentally resonant reaction has a large cross section which has been measured previously by ourselves (Ref. 1) and other workers (Refs. 6,7). All the previous measurements are in good agreement and this reaction, therefore, serves well as a calibration standard.

The apparatus described above is basically the same as that used for our previous measurements (Ref. 1), but some improvements have been made which lower the detection limit for cross section measurements. The major change made was an upgrade of the magnet on the primary mass spectrometer in the system. The upgrade involved replacement of the original electromagnet by a larger coil with a smaller gap. This improvement enables us to get larger primary ion currents since higher ion energies can be used to mass select the primary ions. This improvement has allowed us to lower our upper limit for detectable signals by a factor of approximately two.

Other improvements in the system have included remounting of the collision chamber and lens systems to ensure more accurate alignment.

3. FORMATION OF THE NEUTRAL BEAMS

Beams of neutral particles in our apparatus are made by effusion of a gas or vapor from a small hole in a tube or furnace (see Figure 1). The beam is collimated by two slits in the wall of the separate vacuum chambers employed. Electrically charged plates between the two walls sweep out any ions formed in the furnace. After passing into the experimental chamber, the beam is modulated at 100 Hz by a mechanical chopper.

In our usual mode of operation, the beam density is determined using the cosine law of molecular effusion where the temperature and pressure of the source, the area of the aperture in the tube, and the distance from the source to the interaction region are known factors. This was the technique used when beams of N_2 and O_2 were employed. A more extensive discussion on the determination of the beam density is given in reference 2.

Three sources of O atoms have been employed during the course of our studies of reaction (1). These sources are: thermal dissociation of O_2 in an iridium furnace, rf discharge of mixtures containing principally O_2 molecules and microwave discharge in similar mixtures. The techniques are described below.

3.1 THERMAL DISSOCIATION

Neutral atomic oxygen was formed by thermal dissociation of pure molecular oxygen in an iridium tube furnace. This technique is similar to that first reported by Fite and Irving (Ref. 8). Thermal dissociation has an advantage over other methods for formation of O atoms such as an rf discharge because problems due to metastable O and O_2 particles in the beam are eliminated.

The major difficulty encountered in the thermal dissociation of the oxygen beam is the low beam density obtained. To get a significant dissociation fraction, it was necessary to use low molecular oxygen pressure in the tube furnace. Pressures of the order of 0.06 torr were employed. At these pressures, dissociation fractions of up to 20% were obtained when the furnace was heated to

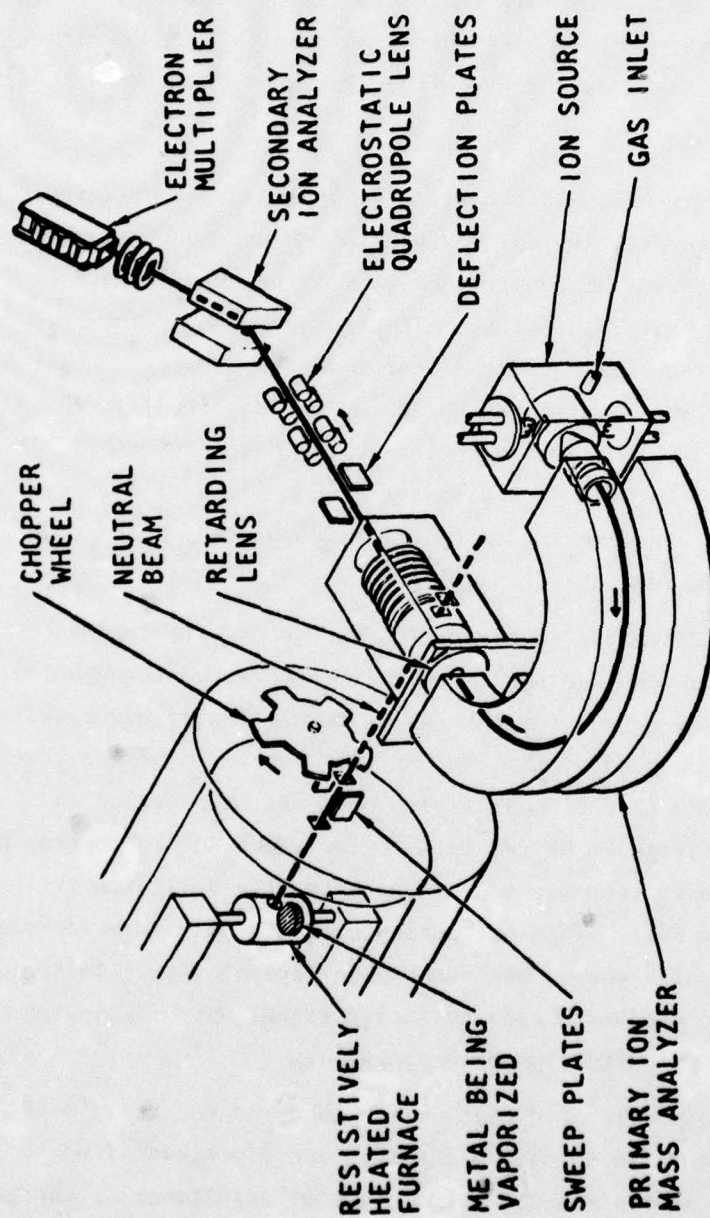


Figure 1. Crossed-ion and neutral-beam apparatus

2100°K. (The furnace temperature was measured using an optical pyrometer.) The resultant atom-beam density in the collision region was approximately 10^9 atoms/cm³. When calculating this beam density, all necessary corrections were made for the atom velocity and the decrease in the O₂ beam density.

3.2 THE rf DISCHARGE

For studies involving discharges, the normal tube or furnace shown as the beam source in Figure 1 is replaced by a discharge tube. For the rf dissociation studies, two different discharge tube geometries were employed. The first was a 20 mm U-shaped pyrex glass tube. The neutral beam is formed by effusion from a small hole in the outside of the bottom of the U-bend. The rf power was supplied by a 50 MHz supply and the energy was coupled in a gas mixture through a copper band fastened around each leg of the discharge tube. The gas mixture was primarily molecular oxygen with trace quantities of water vapor and molecular hydrogen. This arrangement gave a diffuse discharge which produced atomic oxygen but in rather low quantities.

The second discharge tube employed for the rf studies was a 7 mm quartz tube sealed at one end. A small hole was sandblasted through the sealed end to serve as a port of egress for the gas mixture. The rf power was supplied by the same source as used in the case of the U-tube. A unique feature of this discharge tube was that it possessed a bend near the sealed end. This bend allowed the discharge to be run in a region where no high energy photons produced could exit from the source and enter the collision region without first striking a wall. This precaution was necessary in performing our experiments since the high energy photons had sufficient energy to ionize gas in the neutral beam and produce a coherent noise signal which caused an increase in the lower limit for detection of a signal.

Using a phosphoric acid coat on the tube and the gas mixture described above, it was possible to obtain dissociation fractions of up to 40% when the pressure in the source was 0.3 torr. Careful adjustment of the gas mixture allowed the degree of dissociation to be maximized. The amount of O present in the beam was peaked by observing the signal for reaction (7). A dissociation fraction of 40% corresponds to an atomic oxygen beam density of approximately 2×10^{10} atoms/cm³ which is a factor of 20 better than with thermal dissociation. When the rf discharge was being used, it was found that care had to be taken

to eliminate rf pickup in the sensitive detection system used for measurement of the secondary ions. Spurious signals were recorded if this care was not exercised.

3.3 THE MICROWAVE DISCHARGE

The studies using a microwave discharge as a source of O atoms were performed using the bent quartz tube described above in the rf studies section. The microwave power was supplied by a 100W raytheon Microtherm unit operating at 2450 MHz. The microwave power was coupled through the vacuum wall using type N connectors. Inside the vacuum system the power was conducted to the discharge region using semi-rigid coaxial cable. The discharge occurred inside an Evenson type cavity through which the quartz tube passed. This cavity was specially constructed to fit into the restricted volume of our neutral beam source chamber. The microwave discharge operated in much the same manner as the rf case and suffered from the same problems such as high energy photon products. There was some indication that the number of metastable states produced by the microwave discharge was greater than the number produced in the rf case. As a consequence, most of the work using a discharge has been performed using the rf power source.

4. RESULTS TO DATE AND DISCUSSION

4.1 THE CHARGE TRANSFER REACTION $N^+ + O \rightarrow N + O^+$ (REACTION 1)

In our earlier work on reaction (1) (Ref. 2), we used thermal dissociation of O_2 molecules in a heated iridium tube to form our O atom beam. Here there are few complications in that the only species emitted from the source are molecular oxygen (with some vibrational excitation), atomic oxygen, and low energy photons. As such, this would seem to be the ideal source for study of atomic oxygen reactions. The problems that was encountered here was the low dissociation fraction which was obtained and the low O_2 pressure which had to be used to achieve that dissociation fraction.

The low O atom density obtained from the thermal source led us to use the discharge source described in Section 2 in which higher pressures and dissociation fractions could be realized. The major problem one encounters with a discharge is that a variety of species can be formed and will be emitted from the source. These species include unknown quantities of high energy photons, ions, metastable molecules and atoms. The high energy photons were removed by placing a bend in the discharge tube and the ions were swept out of the beam by an electrostatic field in the middle chamber of the vacuum system. The remaining mixture of metastables and atoms led to two problems. The first is the problem of determining the density of the O atoms in the beam, and the second is determining the effect of metastable states on the measured cross section. As mentioned above, the first of these problems was overcome by using the accidentally resonant charge transfer process between H^+ and O [reaction (2)] as a calibrating reaction to determine the O atom density. The use of this reaction, the cross section of which has been measured by several workers (Ref. 1,6,7), eliminates both the problem of determining the O atom density and establishing the collection efficiency for O^+ .

The second problem is more difficult to circumvent and it has been the resolution of this problem which has been the major accomplishment under the task. The problem can be illustrated using the following example. Even without the discharge on, a competing reaction is



This reaction is exothermic and even though its cross section is small, it leads to the formation of O^+ if there is some O_2 in the beam. Using the thermal dissociation source, the effect of this reaction could be accounted for by measuring the cross section for reaction (8) with the source cooled to the point where no dissociation takes place and then heating the source, determining the amount of dissociation occurring and subtracting the appropriate amount from the O^+ signal registered.

With a discharge source the problem is not this simple. Here you have the possibility of forming a substantial amount of the $\text{O}_2(^1\Delta)$ metastable in the discharge. If the cross section for reaction (8) is different when O_2 is in the ground state or the metastable state, which it may well be, the method of correction described above is no longer valid and different techniques must be employed.

There are two ways to approach this problem. The first is to find a gas to flow through the discharge tube which will produce O atoms but has no other component which leads to O^+ ions in the reaction region. In our studies we have attempted to form O atoms by discharges in CO_2 . The results with the CO_2 discharges appeared to be very similar to those obtained with O_2 which are described below.

The second possible way around the problem is to attempt to determine the effect of $\text{O}_2(^1\Delta)$ present in the beam formed by a discharge in O_2 . We have attempted to do this by running a discharge in pure O_2 in a clean quartz tube which is not coated with phosphoric acid. Such a system gives very little dissociation but appears to give up to 20% $\text{O}_2(^1\Delta)$ (Ref. 9). The result of this experiment is that the amount of O^+ formed in the beam by reaction (8) with the discharge off is slightly less than that formed with the discharge on. The cross section for formation of O^+ by reaction (8) is therefore relatively independent of the state of the O_2 but, nevertheless, the signals for reaction (1) were so small that this effect could not be ignored.

In order to illustrate the complexity of the measurements that had to be employed to obtain the needed data, the procedure employed for each point is given.

1. Establish a stable ion and neutral beam. The neutral beam must be stable both when the rf discharge is off (no O atoms) and on (O atoms present). In order to ensure a stable discharge with significant O atom density present, it was necessary to have the discharge operating in the correct mode and with the proper gas mixture. The mode of operation was established by visual observation of the discharge color. A fiber optics link was used for this purpose. The gas mixture giving the highest dissociation was found to be pure O_2 containing 2% water vapor and 1% hydrogen. The degree of dissociation was further enhanced by treating the quartz discharge tube with dilute phosphoric acid.
2. Measure the signal for the reaction $N^+ + O_2 \rightarrow N + O_2^+$ with both discharge on and discharge off. Determination of the decrease in signal when the discharge is struck is one method of determining the amount of O_2 dissociated, and, hence, the oxygen atom density in the beam. Great care must be exercised in interpreting the results; however, since the presence of O_2^+ formed in the discharge may influence the results. This problem was discussed above.
3. Measure the signal for the reaction $N^+ + O_2 \rightarrow NO^+ + O$ with both discharge on and discharge off. This step gives the same information as step 2 but is suspect for the same reason. It should be noted, however, that the dissociation fractions determined in steps 2 and 3 usually agreed to within a few percent.
4. Measure the signal for the reaction $H^+ + O \rightarrow H + O^+$ with the discharge on. Since the cross section for this reaction is known (Refs. 1,6,7), this measurement gives a means of establishing in the system gain and collection efficiency for O^+ ions formed

by charge transfer. If these factors are known, then this procedure ultimately gives another measurement of the oxygen atom density in the beam.

5. Measure the signal for the reaction $N^+ + O_2 \rightarrow NO + O^+$ with both discharge off and discharge on. The dissociation fraction determined in 2, 3, and 4 above, is used to calculate the decrease which should be expected in the signal for the reaction due to the decrease in O_2 density when the discharge is struck. Any difference between the expected signal size and the measured signal size is due to the signal for the desired reaction $N^+ + O \rightarrow N + O^+$ [reaction (1)]. This difference signal is compared with the signal for $H^+ + O \rightarrow H + O^+$ to determine the absolute magnitude of the cross section.

Since the signal differences between the obtained and expected signals for 5 above were small fractions of the signals measured, considerable scatter was often encountered and, as a consequence, many measurements had to be made at each energy under identical conditions.

The major uncertainty in the measurements was that when the discharge was struck, other species such as $O_2(a^1\Delta_g)$ would be produced in the neutral beam and interfere with the measurements. As discussed above, by varying the amount of dissociation in the discharge tube, it was possible to make an allowance for the presence of this species.

The data obtained for the charge transfer between N^+ and O, reaction (1), is given in Table I. As mentioned above, there is considerable scatter in the values obtained. The cross section given at each energy in the table is in most cases the average of several determinations. Examination of the data in the table shows that the cross section for the reaction is relatively flat over the energy range considered (0.5 eV to 12 eV in the center-of-mass system). The value of the cross section at the lowest energy used is approximately $1.2 \times 10^{-17} \text{ cm}^2$ and increases slowly to about $2.5 \times 10^{-17} \text{ cm}^2$ at the upper end of the energy range.

Table I. Charge transfer cross sections for the reaction
 $N^+ + O \rightarrow N + O^+$

ION LAB ENERGY (EV)	COLLISION ENERGY (EV)	CROSS SECTION (CM ²)	RATE COEFFICIENT (CM ³ /SEC)	ION VELOCITY (CM/SEC)	RELATIVE VELOCITY (CM/SEC)
0.93	52	1.220-17	4.462-12	3.581+05	3.657+05
1.00	55	9.300-18	3.522-12	3.713+05	3.787+05
1.25	69	1.360-17	5.736-12	4.152+05	4.218+05
1.14	63	3.300-17	1.331-11	3.965+05	4.034+05
1.46	80	7.500-18	3.411-12	4.487+05	4.548+05
1.53	84	1.960-17	9.120-12	4.593+05	4.653+05
1.93	100	1.250-17	6.348-12	5.023+05	5.078+05
1.96	107	1.200-17	6.302-12	5.199+05	5.252+05
2.00	109	1.770-17	9.388-12	5.251+05	5.304+05
2.25	122	1.970-17	1.107-11	5.570+05	5.619+05
2.50	135	2.320-17	1.373-11	5.871+05	5.918+05
2.73	148	2.240-17	1.384-11	6.135+05	6.180+05
2.80	151	2.150-17	1.345-11	6.214+05	6.258+05
3.00	162	1.640-17	1.062-11	6.432+05	6.475+05
3.18	172	3.100-17	2.066-11	6.622+05	6.663+05
3.50	189	1.800-17	1.258-11	6.947+05	6.987+05
4.00	215	2.250-17	1.679-11	7.427+05	7.464+05
4.50	242	2.180-17	1.725-11	7.877+05	7.912+05
5.00	269	2.100-17	1.751-11	8.303+05	8.336+05
5.46	307	1.970-17	1.865-11	9.438+05	9.467+05
6.40	363	1.150-17	1.312-11	1.138+06	1.141+06
14.40	770	2.600-17	3.669-11	1.409+06	1.411+06
19.35	1038	2.440-17	3.990-11	1.633+06	1.635+06
24.30	1298	2.250-17	4.122-11	1.830+06	1.832+06

4.2 THE REACTIONS OF Al^+ WITH O_2 AND N_2

The following reactions of Al^+ with O_2 and N_2 have been reinvestigated



The energy range was 1 eV to 5000 eV ion energy.

The purpose of this reinvestigation was to check our previous results in an attempt to explain why our cross section data did not explain the results obtained in a related experiment conducted at TRW by Friichtenicht and co-workers. One suggestion they made was that we were not collecting all the product formed in the collisions. In our remeasurement of the cross sections, great care was taken to ensure total collection of the product by the application of stronger than normal extraction fields across the collision region. These tests, in which the field was applied until saturation was obtained, indicated no significant change in the measured cross sections for the ion-molecule reaction [reactions (2)]. As in the previous work, no cross section could be measured for reaction (4). For the charge transfer processes [reactions (3) and (5)], some change in the curve shape when compared to our previous data was observed but the values were within the error limits previously assigned.

The results for reaction (2) are shown in Figure 2. The process shows a threshold for reaction indicating its endothermic nature. This reaction has a maximum cross section of $5.5 \times 10^{-17} \text{ cm}^2$ at approximately 9 eV ion energy. For reaction (4) an upper limit of approximately 10^{-18} cm^2 has been established over the total energy range considered.

Signals for the charge transfer, reactions (3) and (5), could only be detected at high energies (above 1000 eV ion energy). The results are shown in Figure 3. Both cross sections are observed to rise in the high energy region and are still increasing at 5000 eV, the highest ion energy employed. At this energy, reaction (3) had a cross section of $1.3 \times 10^{-17} \text{ cm}^2$ and reaction (5) of $1.2 \times 10^{-17} \text{ cm}^2$. In our experiment these cross sections could not, of course, be distinguished from those resulting from ionization of the O_2 and N_2 by Al^+ .

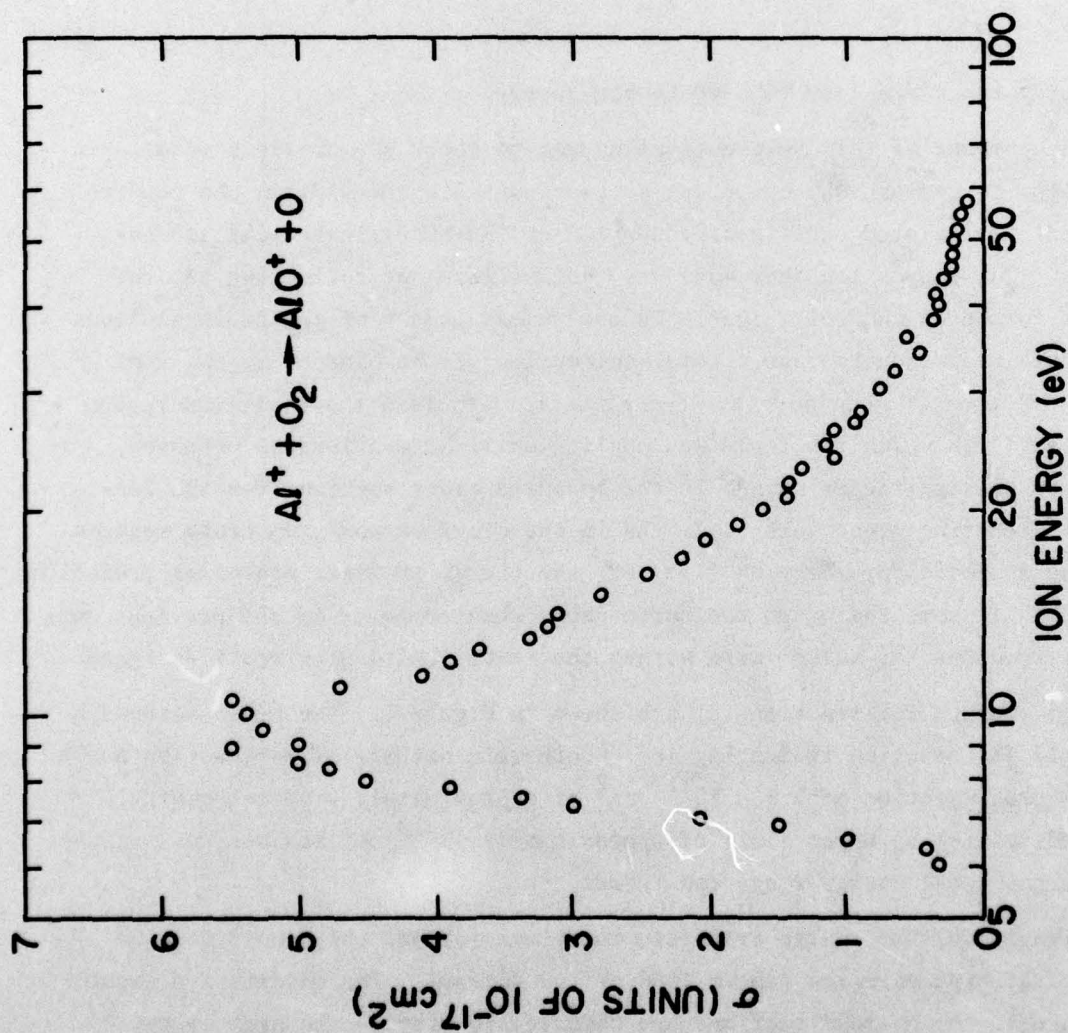


Figure 2. Cross section for the ion-molecule reaction $\text{Al}^+ + \text{O}_2 \rightarrow \text{AlO}^+ + \text{O}$ as a function of the ion energy

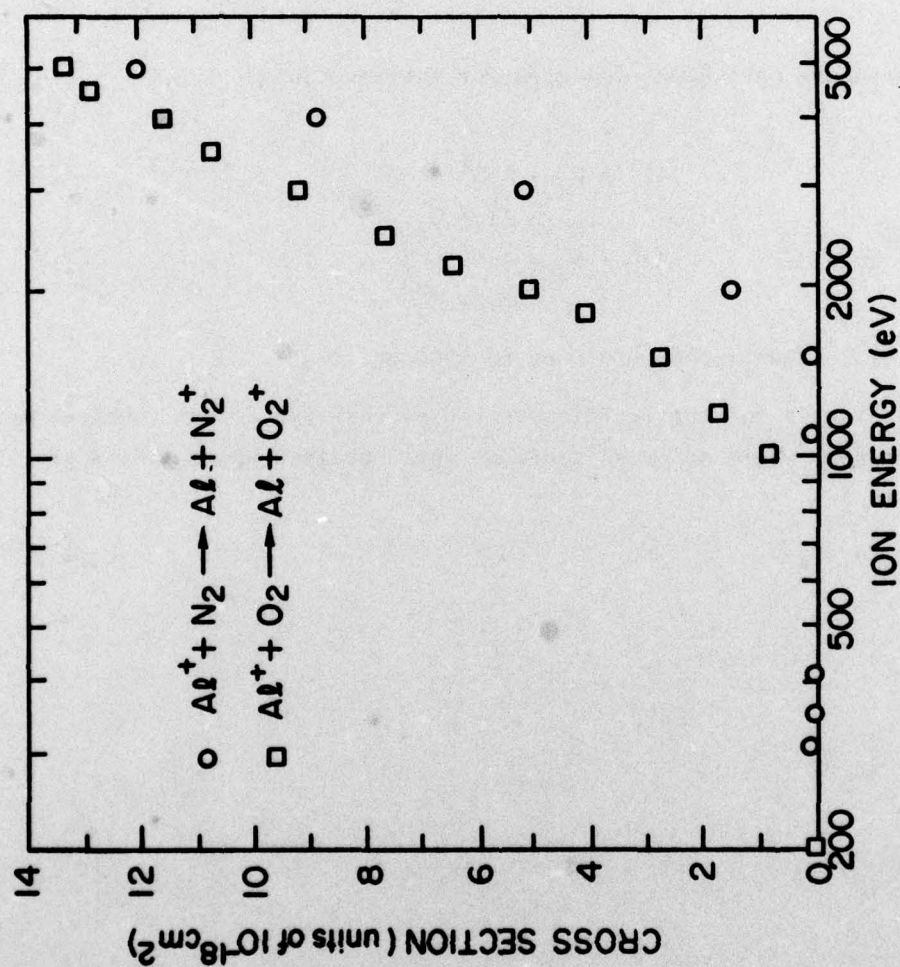
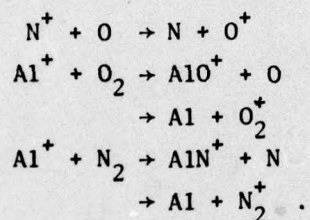


Figure 3. Cross sections for the charge-transfer reactions $\text{Al}^+ + \text{N}_2 \rightarrow \text{Al} + \text{N}_2^+$ (o) and $\text{Al}^+ + \text{O}_2 \rightarrow \text{Al} + \text{O}_2^+$ (\square) as a function of the ion energy

Attempts were made to detect the products of dissociative charge transfer. No signals for O^+ or N^+ could be detected and an upper limit of $5 \times 10^{-19} \text{ cm}^2$ over the entire energy range has been established.

5. SUMMARY

Measurements have been completed for the reactions



for ion energies ranging from 0.5 eV to 5000 eV.

Where signals for the reactions could be observed, cross sections have been determined; where no cross sections were obtained upper limits are given.

REFERENCES

1. J. A. Rutherford and D. A. Vroom, "The Reaction of Atomic Oxygen with Several Atmospheric Ions," J. Chem. Phys. 61, 2514 (1974).
2. J. A. Rutherford and D. A. Vroom, "Ion-Neutral Reactions of Al^+ with N_2 , O_2 , and N_2O ," J. Chem. Phys. 65, 4445 (1976).
3. J. A. Rutherford, R. F. Mathis, B. R. Turner, and D. A. Vroom, "Formation of Magnesium Ions by Charge Transfer," J. Chem. Phys. 55, 3785 (1971).
4. R. F. Stebbings, B. R. Turner, and J. A. Rutherford, "Low-Energy Collisions Between Some Atmospheric Ions and Neutral Particles," J. Geophys. Res. 71, 771 (1966).
5. B. R. Turner, J. A. Rutherford, and R. F. Stebbings, "Charge Transfer Reactions of Nitric Oxide and Atomic and Molecular Ions of Oxygen and Nitrogen," J. Geophys. Res. 71, 4521 (1966).
6. R. F. Stebbings, A. C. H. Smith, and H. Ehrhardt, "Charge Transfer Between Oxygen and O^+ and H^+ Ions," J. Geophys. Res. 69, 2349 (1964).
7. F. C. Fehsenfeld and E. E. Ferguson, "Thermal Energy Reaction Rate Constants for H^+ and CO^+ with O and NO," J. Chem. Phys. 56, 3066 (1972).
8. W. L. Fite and P. Irving, "Chemi-ionization in Collisions of Uranium Atoms with Oxygen Atoms and Molecules," J. Chem. Phys. 56, 4227 (1972).
9. P. D. Burrow, "Dissociative Attachment from the $O_2(a^1\Delta_g)$ State," J. Chem. Phys. 59, 4922 (1973).

DISTRIBUTION LIST

DEPARTMENT OF DEFENSE

Assistant to the Secretary of Defense
Atomic Energy
ATTN: Executive Assistant

Defense Advanced Rsch. Proj. Agency
ATTN: TIO

Defense Documentation Center
12 cy ATTN: DD

Defense Nuclear Agency
ATTN: DDST
2 cy ATTN: RAAE
4 cy ATTN: TITL

Field Command
Defense Nuclear Agency
ATTN: FCPR

Field Command
Defense Nuclear Agency
Livermore Division
ATTN: FCPRL

Interservice Nuclear Weapons School
ATTN: TTV

Under Secy. of Def. for Rsch. & Engrg.
ATTN: Strategic & Space Systems (OS)

DEPARTMENT OF THE ARMY

Atmospheric Sciences Laboratory
U.S. Army Research & Development Command
ATTN: H. Ballard
ATTN: M. Hepps
ATTN: DELAS-AE-M, F. Niles

BMD Advanced Technology Center
Department of the Army
ATTN: ATC-O, W. Davies
ATTN: ATC-T, M. Capps

Harry Diamond Laboratories
Department of the Army
ATTN: DELHD-N-NP
ATTN: DELHD-I-TL, N. Brandt

U.S. Army Ballistic Research Labs
ATTN: M. Kregel
ATTN: Technical Library
ATTN: DRDAR-BLB, G. Keller
ATTN: DRDAR-BLB, J. Heimerl
ATTN: J. Vanderhoff

U.S. Army Missile R&D Command
ATTN: Redstone Scientific Information Center

U.S. Army Nuclear & Chemical Agency
ATTN: Library

U.S. Army Research Office
ATTN: R. Mace

DEPARTMENT OF THE ARMY (Continued)

U.S. Army Foreign Science & Tech. Ctr.
ATTN: DRXST-SD3, J. Tobias

U.S. Army TRADOC Systems Analysis Activity
ATTN: ATAA-PL

White Sands Missile Range
Department of the Army
ATTN: STEWS-TE-AN, M. Squires

DEPARTMENT OF THE NAVY

Naval Electronic Systems Command
ATTN: ELEX 03
ATTN: PME 117-T

Naval Intelligence Support Ctr.
ATTN: Document Control

Naval Ocean Systems Center
ATTN: Code 4471
ATTN: Code 532, R. Pappert
ATTN: Code 5321, I. Rothmuller
ATTN: Code 5324, W. Moler
ATTN: Code 5322, H. Hughes
ATTN: Code 532, J. Richter

Naval Research Laboratory
ATTN: Code 2627
ATTN: Code 7175, J. Johnson
ATTN: Code 6709, W. Ali
ATTN: Code 1434, E. Brancato
ATTN: Code 6750, D. Strobel
ATTN: Code 6701, J. Brown
ATTN: Code 7120, R. Kinzer
ATTN: Code 6780, S. Ossakow
ATTN: Code 7122, D. McNutt
ATTN: Code 7750, J. Fedder
ATTN: Code 6750, K. Hain
ATTN: Code 6707, J. Davis
ATTN: Code 7175H, D. Horan
ATTN: Code 7101, P. Mange
ATTN: Code 6700, T. Coffey

Nuclear Weapons Tng. Center Pacific
Department of the Navy
ATTN: Nuclear Warfare Department

Office of Naval Research
ATTN: Code 465, G. Joiner
ATTN: Code 421, B. Junker

Naval Surface Weapons Center
White Oak Laboratory
Code F31
ATTN: L. Rudlin
ATTN: Doce R41, D. Land
ATTN: Code F46, D. Hudson

DEPARTMENT OF THE AIR FORCE

Air Force Weapons Laboratory, AFSC
ATTN: SUL

DEPARTMENT OF THE AIR FORCE (Continued)

Air Force Geophysics Laboratory, AFSL

ATTN: LKB, F. Innes
ATTN: OPRI, J. Ulwick
ATTN: LKB, K. Champion
ATTN: LKO, R. Huffman
ATTN: LKD, C. Philbrick
ATTN: LKB, J. Paulson
ATTN: OP, J. Garing
ATTN: LKB, T. Keneshea
ATTN: LKD, R. Narcisi
ATTN: LKB, W. Swider, Jr.
ATTN: LKB, E. Murad
ATTN: OPR, A. Stair
ATTN: OPR, H. Gardiner
ATTN: OPR, F. Delgreco
ATTN: OPR, R. O'Neill
ATTN: OPR, J. Kennealy
ATTN: OPR, T. Connolly
ATTN: SULL
ATTN: LKO, R. Vantassel

Air Force Technical Applications Center

ATTN: TD
ATTN: STINFO Office/TF
ATTN: TF/Capt Seiler

Foreign Technology Division, AFSC

ATTN: WE
ATTN: NIIS Library

Rome Air Development Center, AFSC

ATTN: OCS, V. Coyne

U.S. Air Force Environmental
Technical Applications Center

ATTN: CBTL

DEPARTMENT OF ENERGY

Department of Energy

ATTN: H. Kurzweg

OTHER GOVERNMENT AGENCIES

Bureau of Mines

Pittsburgh Mining & Safety Rsch. Ctr.
ATTN: J. Murphy

Department of Commerce

National Bureau of Standards

ATTN: A. Phelps
ATTN: W. Lineberger
ATTN: S. Leone

Department of Commerce

National Bureau of Standards

ATTN: J. Devoe
ATTN: J. Cooper
ATTN: M. Scheer
ATTN: R. Hampson, Jr.
ATTN: M. Krauss
ATTN: D. Lide
ATTN: D. Garvin
ATTN: L. Gevantman
ATTN: S. Abramowitz

Department of Commerce

National Oceanic & Atmospheric Admin.
ATTN: Assistant Administrator, RD

OTHER GOVERNMENT AGENCIES (Continued)

Department of Commerce

National Oceanic & Atmospheric Admin.
Environmental Research Laboratories

ATTN: E. Ferguson
ATTN: G. Reid
ATTN: F. Fehsenfeld
ATTN: W. Spjeldvik
ATTN: D. Albritton

Department of Transportation

Transportation Rsch. System Center
ATTN: F. Marmo

NASA

Goddard Space Flight Center

ATTN: Technical Library
ATTN: M. Sugiyra
ATTN: J. Vette
ATTN: A. Aiken
ATTN: S. Bauer

NASA

George C. Marshall Space Flight Center

ATTN: W. Roberts

NASA

ATTN: N. Roman
ATTN: F. Schmerling
ATTN: R. Schiffer
ATTN: D. Denent

NASA

Johnson Space Center

ATTN: Classified Lib., Code JM6

NASA

Ames Research Center

ATTN: W. Starr
ATTN: R. Whitten
ATTN: G. Poppoff

National Science Foundation

ATTN: R. Sinclair
ATTN: A. Grobecker
ATTN: R. McNeal

DEPARTMENT OF DEFENSE CONTRACTORS

Aero-Chem. Research Labs, Inc.

ATTN: A. Fontijn

AeroDyne Research, Inc.

ATTN: F. Bien
ATTN: M. Camac
ATTN: Librarian
ATTN: M. Faist

Aerospace Corp.

ATTN: R. Cohen
ATTN: Library
ATTN: M. Whitson
ATTN: T. Taylor
ATTN: H. Mayer
ATTN: L. Brary

Avco Everett Research Lab., Inc.

ATTN: C. Von Rosenberg, Jr.

Berkeley Research Associates, Inc.

ATTN: J. Workman

DEPARTMENT OF DEFENSE CONTRACTORS (Continued)

Boston College
ATTN: F. McElroy
ATTN: D. McFadden

University of California at San Diego
Dept. of Applied Mech. & Engrg. Sciences
ATTN: D. Miller

University of California at Santa Barbara
Physics Department
ATTN: M. Steinberg

California Institute of Technology
Jet Propulsion Lab
ATTN: S. Trajmar
ATTN: V. Anicich

University of California
Berkeley Campus
ATTN: H. Johnston

Calspan Corp.
ATTN: C. Treanor
ATTN: W. Wurster
ATTN: Library

Chem Data Research
ATTN: K. Schofield

Columbia University
Low Memorial Library
ATTN: H. Foley

University of Denver
Colorado Seminary
Denver Research Institute
ATTN: Sec. Officer for Van Zyl
ATTN: Sec. Officer for D. Murcray

Epsilon Labs, Inc.
ATTN: C. Accardo

ESL, Inc.
ATTN: W. Bell

EG&G, Inc.
Los Alamos Division
ATTN: P. Lucero

General Dynamics Corp.
ATTN: Convair Research Library

General Electric Co.
Space Division
ATTN: R. Edsall
ATTN: Technical Information Center
ATTN: P. Zavitsanos
ATTN: J. Peden
ATTN: J. Burns
ATTN: M. Lineusky
5 cy ATTN: T. Baurer
6 cy ATTN: M. Bortner

General Electric Company
Corporate Research & Development Ctr.
ATTN: J. Schroeder

DEPARTMENT OF DEFENSE CONTRACTORS (Continued)

General Electric Company-TEMPO
Center for Advanced studies
ATTN: M. Stanton
ATTN: T. Stevens
ATTN: L. Ewing
ATTN: W. Knapp
ATTN: M. Dudash
ATTN: D. Reitz
ATTN: D. Chandler
ATTN: B. Gambill
ATTN: J. Thompson
ATTN: DASIAC

General Research Corp.
Santa Barbara Division
ATTN: J. Ise, Jr.

General Research Corp.
ATTN: T. Zakrzewski

Geophysical Institute
University of Alaska
ATTN: R. Parthasarathy
ATTN: N. Brown

HSS, Inc.
ATTN: D. Hansen
ATTN: M. Shuler

Hughes Aircraft Co.
ATTN: Tech, B. Campbell

Information Science, Inc.
ATTN: W. Dudziak

Institute for Defense Analyses
ATTN: F. Bauer
ATTN: H. Wolfhard

Ion Physics Corp.
ATTN: C. Hauer

IRT Corp.
ATTN: D. Vroom
ATTN: R. Neynaber
ATTN: R. Overmyer
ATTN: J. Rutherford

Johns Hopkins University
Applied Physics Lab.
ATTN: Document Library

Johns Hopkins University
ATTN: J. Kaufman

Kaman Sciences Corp.
ATTN: W. Rich
ATTN: D. Foxwell

KMS Industries, Inc.
ATTN: Library

Los Alamos Scientific Laboratory
ATTN: J. Malik
ATTN: W. Hughes
ATTN: W. Barfield
ATTN: J. Zinn
ATTN: H. Hoerlin

DEPARTMENT OF DEFENSE CONTRACTORS (Continued)

Lockheed Missiles and Space Co., Inc.

ATTN: B. McCormac
ATTN: J. Kumer
ATTN: M. Walt
ATTN: R. Sears
ATTN: R. Gunton
ATTN: T. James
ATTN: J. Reagan
ATTN: J. Evans

University of Lowell
Center for Atmospheric Research
ATTN: G. Best

University of Maryland
ATTN: J. Vanderslice

University of Minnesota
ATTN: J. Winkler

University of Minnesota
ATTN: M. Hirsch

Mission Research Corp.
ATTN: R. Kilb
ATTN: W. White
ATTN: R. Hendrick
ATTN: M. Scheibe
ATTN: M. Messier
ATTN: V. Van Lint
ATTN: D. Sappenfield
ATTN: D. Archer

University of Massachusetts
Astronomy Research Facility
ATTN: H. Sakai

M.I.T. Lincoln Lab.
ATTN: B. Watkins

National Academy of Sciences
National Materials Advisory Board
ATTN: J. Sievers

State University of New York at Buffalo
Nuclear Science & Technology Facility
ATTN: G. Brink

Pacific-Sierra Research Corp.
ATTN: F. Field, Jr.

Pennsylvania State University
Industrial Security Office
ATTN: J. Nisbet
ATTN: L. Hale

Photometrics, Inc.
ATTN: I. Kofsky

Physical Dynamics, Inc.
ATTN: A. Thompson

Physical Science Lab.
ATTN: W. Berning

Physical Sciences, Inc.
ATTN: K. Wray
ATTN: R. Taylor
ATTN: G. Caledonia

DEPARTMENT OF DEFENSE CONTRACTORS (Continued)

Nichols Research Corp.
ATTN: N. Byrn

Panametrics, Inc.
ATTN: B. Sellers

University of Pittsburgh
Cathedral of Learning
ATTN: M. Biondi
ATTN: W. Fite
ATTN: F. Kaufman

R & D Associates
ATTN: B. Gabbard
ATTN: C. MacDonald
ATTN: R. Turco
ATTN: R. Lelevier
ATTN: F. Gilmore
ATTN: H. Ory

R & D Associates
ATTN: H. Mitchell
ATTN: J. Rosengren
ATTN: B. Yoon

Radiation Research Associates, Inc.
ATTN: N. Schaeffer

Rand Corp.
ATTN: C. Crain

Rice University
Department of Space Science
ATTN: R. Stebbings

Quantum Systems, Inc.
ATTN: S. Ormonde

Rice University
ATTN: J. Chamberlain

Sandia Laboratories
ATTN: W. Brown
ATTN: T. Wright

Science Applications, Inc.
ATTN: D. Hamlin

Science Applications, Inc.
Huntsville Office
ATTN: D. Divis

Science Applications, Inc.
ATTN: R. Johnston

University of Illinois
ATTN: C. Sechrist

Sidney A. Bowhill
ATTN: S. Bowhill

Technology International Corp.
ATTN: W. Boquist

Teledyne Brown Engineering
ATTN: R. Deliberis

University of Texas System
ATTN: J. Browne

DEPARTMENT OF DEFENSE CONTRACTORS (Continued)

SRI International

ATTN: J. Peterson
ATTN: A. Peterson
ATTN: G. Black
ATTN: A. Whitson
ATTN: J. Moseley
ATTN: F. Kindermann
ATTN: M. Baron
ATTN: D. Hildenbrand
ATTN: R. Hake, Jr.
ATTN: R. Leadabrand
ATTN: T. Slanger
ATTN: V. Wickwar

TRW Defense & Space Sys. Group

ATTN: J. Frichtenicht
ATTN: Technical Information Center

Utah State University

ATTN: Security Officer for K. Baker

University of Virginia

School of Engineering & Appl. Sciences
Rsch. Labs of the Engineering Sciences

ATTN: R. Ritter
ATTN: H. Kelly
ATTN: R. McKnight

DEPARTMENT OF DEFENSE CONTRACTORS (Continued)

Visidyne, Inc.

ATTN: T. Degges
ATTN: H. Smith
ATTN: C. Humphrey
ATTN: J. Carpenter

Wayne State University

ATTN: R. Kummier
ATTN: P. RoI

University of Washington

ATTN: K. Clark

Westinghouse Electric Corp.

Research and Development Center
ATTN: P. Chantry